Peptide Nanowires

DOI: 10.1002/ange.201003446

Self-Assembly of Semiconducting Photoluminescent Peptide Nanowires in the Vapor Phase**

Joon Seok Lee, Ilsun Yoon, Jangbae Kim, Hyotcherl Ihee, Bongsoo Kim,* and Chan Beum Park**

The self-assembly of bioorganic molecules, which are ubiquitous in nature, is an attractive route for fabricating functional supramolecular architectures.[1] It also facilitates the preparation of highly ordered nanostructures by the organization of molecular building blocks through the combination of noncovalent interactions including hydrogen bonds, electrostatic interactions, π–π stacking, hydrophobic interactions, and dipole–dipole interactions.[2–5] The fabrication of nanostructures through the self-assembly of peptides has attracted interest because of the unique properties of peptides, such as their functional flexibility and molecular recognition capability.[6–12] In particular, the self-assembly of an aromatic dipeptide consisting of two covalently linked phenylalanine units (namely, diphenylalanine, FF), which is a key structural motif in Alzheimer's β-amyloid polypeptides, serves as an excellent model because it can spontaneously form various nanostructures in aqueous or organic environments.[13]

Herein, we report the first synthesis of semiconducting, single-crystalline, peptide-based nanowires (NWs) through a simple vapor-transport process as well as the characterization of their molecular arrangement. Single-crystalline NWs were synthesized through a simple vapor-transport process in which the linear FF peptide was used as the starting material. Powdered FF was vaporized at 250 °C in an argon atmosphere and transported downstream in a horizontal tube (see Figure S1 in the Supporting Information). Thermogravimetric analysis (TGA) shows that the peptide powder begins to vaporize at approximately 250 °C (Figure S2a). Peptide NWs were grown on a silicon substrate located downstream at 180 °C. The as-synthesized peptide NWs were well-faceted with a smooth surface and an average diameter of approximately 90 nm (Figure 1 a). A gradual growth of peptide NWs occurs during the vapor-transport process (Figure S3): after the formation of nuclei on the substrate, short peptide fibrils grow into peptide NWs that are longer than 10 μm. No additional mass loss was observed by TGA up to 250 °C, which indicates a high thermal stability of the synthesized peptide NWs (Figure S2b). Figure 1 b shows a selected-area electron-diffraction (SAED) pattern of a representative single peptide NW. The SAED pattern of the NW exhibits a regular spot pattern, thus indicating that the peptide NW is single-crystalline.

To investigate the crystal structure of the peptide NW a finely ground sample of the peptide NW was analyzed by powder X-ray diffraction (PXRD) at room temperature (Figure S4). Most reports previously suggested that the crystal structure of self-assembled FF nanostructures consisted of an ordered hexagonal array of normal linear dipeptide molecules.[14–16] According to our results, the vapor-transport process converted linear FF into cyclo-FF, in which the terminal carboxylic acid and amine groups fused together during evaporation to form a cyclic amide bond—namely, 3,6-bis(phenylmethyl)-2,5-piperazinedione (cyclo-FF)—and with aromatic stacking between the side chains. According to the literature,[17–21] dipeptides can lose water and form cyclic analogues upon heating. To unravel the molecular arrangement of NWs we performed Pawley refinement to optimize the lattice parameters and, subsequently, carried out Rietveld refinements (Figure S4) using the single-crystal structure of cyclo-FF[22] and considering all the possible geometrical degrees of freedom. The simulated pattern fits well with the experimental PXRD pattern ($R_{wp} = 8.82\,\%$, and $R_P = 6.81\,\%$, respectively) collected by using synchrotron radiation (Pohang Accelerator Laboratory, Korea); the refined lattice parameters [$a = 6.18517(17)$ Å, $b = 10.38349(29)$ Å, $c = 23.85128(62)$ Å] from Rietveld refinement are consistent with the SAED pattern (Figure S4). While TGA showed that the FF powder lost water at around 100 °C, the peptide NWs did not show such a water loss, which indicates that the as-synthesized peptide NWs did not contain water (Figure S2b). The NWs in this study were assembled by a vapor-transport process, with no water molecules involved. The FF molecules in the previously reported linear FF based nanotubes (NTs) assemble around central water clusters through hydrogen bonds to form a hexagonal unit cell in an aqueous environment.[15,16] Vapor-phase processes often pro-

[*] J. S. Lee, Prof. C. B. Park
Department of Materials Science and Engineering, KAIST
Daejeon 305-701 (Korea)
E-mail: parkcb@kaist.ac.kr
I. Yoon, Prof. B. Kim
Department of Chemistry, KAIST
Daejeon 305-701 (Korea)
E-mail: bongsoo@kaist.ac.kr
J. Kim, Prof. H. Ihee
Center for Time-Resolved Diffraction
Department of Chemistry, and Graduate School of Nanoscience & Technology (WCU), KAIST
Daejeon 305-701 (Korea)
E-mail: hyotcherl.ihee@kaist.ac.kr

[**] This study was supported by MEST/NRF, Korea through the NRL (R0A-2008-000-20041-0, 20090083138), SRC (20100001484), CNMT (2010-K000350), Converging Research Center (2009-0082276), Engineering Research Center (2008-0062205), and Creative Research Initiatives (Center for Time-Resolved Diffraction) programs. We thank Docheon Ahn for his help in collecting the PXRD data.

Supporting information for this article is available on the WWW under http://dx.doi.org/10.1002/anie.201003446.

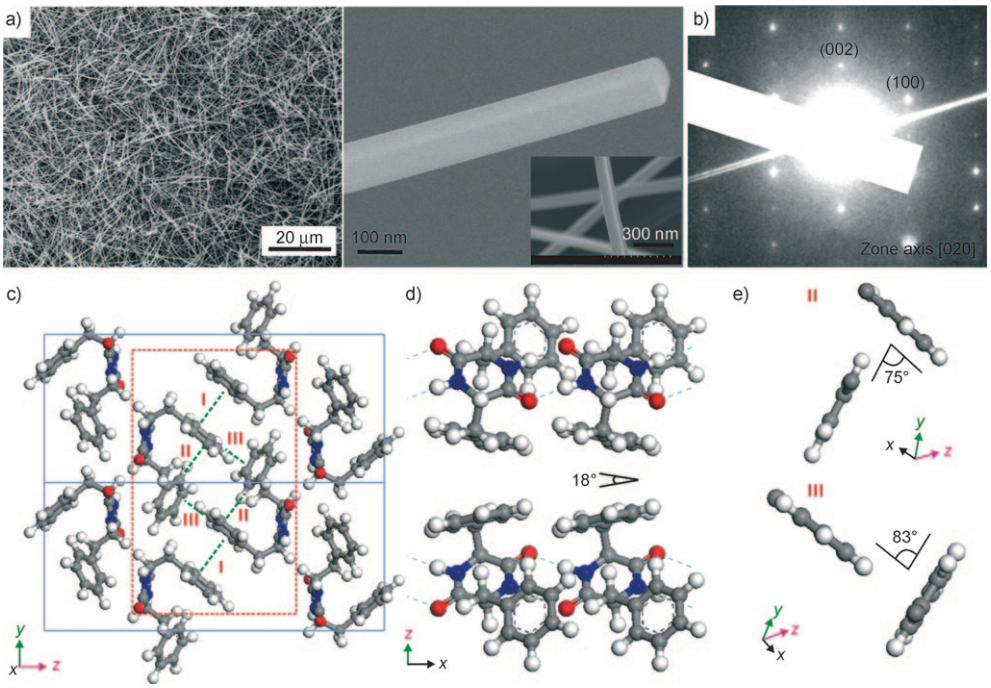

Figure 1. a) Representative SEM images of semiconducting cyclo-FF NWs grown on a Si substrate, b) SAED pattern of a single cyclo-FF NW, and c)–e) molecular arrangements of cyclo-FF dipeptide in NWs with an orthorhombic lattice (pale violet solid line) after Rietveld refinement; c) aromatic stacking (green dotted line, I) and two types of herringbone interaction networks (green dotted lines, II and III) along the *b* axis. d) Intermolecular hydrogen bonds (blue dotted lines, within 2.5 Å) between cyclo-FF dipeptide molecules in NWs along the *x* axis. The angle between facing phenyl rings is 18°. e) The herringbone-type conformations of phenyl rings (II and III) in the red dotted rectangle in (c). The refined lattice parameters from Rietveld refinement are measured to be $a = 6.18517(17)$ Å, $b = 10.38349(29)$ Å, $c = 23.85128(62)$ Å.

duce nanostructures of higher crystallinity than solution-phase processes because the self-assembled crystallization of building blocks in the vapor phase occurs at significantly higher temperatures, with no participating solvent molecules.[23] The detailed molecular arrangement of cyclo-FF molecules in the unit cell is represented in the lower panel of Figure 1, and is characterized by aromatic stacking (Figure 1c; green dotted line; I), two kinds of herringbone interaction (Figure 1c; green dotted lines; II, III) along the *b* axis, and intermolecular hydrogen bonds between carbonyl oxygen atoms and amine hydrogen atoms along the *a* axis (Figure 1d). The aromatic stacking slightly deviates from a parallel geometry, with an angle of 18° between facing phenyl rings, and thus the interaction distances vary from 3.642 to 4.678 Å. The inequivalent herringbone interactions (Figure 1e) show two kinds of angles between the planes of the phenyl rings: 75° and 83° for geometries II and III, respectively. In addition, the C(π)···C(π) distances were measured to be approximately 3.85 Å and 4.07 Å in geometries II and III, respectively.

We characterized the optical properties of the cyclo-FF NWs by using diffuse reflectance spectroscopy (DRS), photoluminescence (PL) spectroscopy, and Raman microscopy on single NWs. Optical-diffusion reflection spectra of the cyclo-FF NWs was measured and compared with those of hexagonal linear-FF nanotubes (NTs) and linear-FF powders. The linear-FF NTs with a hexagonal crystal system were prepared by the reported method.[24,25] Figure 2a shows plots of the Kubelka–Munck remission function versus photon energy, which corresponds to the absorption spectra. The peptide powders, NTs, and NWs all exhibit two strong absorption bands around 220 and 260 nm, which are attributed to phenylalanine.[8] The cyclo-FF NWs, however, show an additional strong band at 306 nm and a weak one at 365 nm; the optical band gap (E_g) of the NWs estimated from the DRS spectra is 3.63 eV (Figure 2a, inset). It has been reported that linear-FF NTs possess a wide band gap ($E_g > 4$ eV) and are electronically insulating.[26,27] Although the presence of aromatic rings in the side chain of NTs can significantly reduce the size of the band gap [2.94 eV for cyclic $(Gln\text{-}Phe)_4$ peptide NTs], a large distance (typically 4.7 Å) between peptides may prevent efficient orbital overlap (3–4 Å) and make peptide NTs poor tunneling conductors.[28]

Figure 2b compares the photoluminescence (PL) spectrum of cyclo-FF NWs with those of linear-FF powders and linear-FF NTs excited at 367 nm. While very weak emission was observed in the visible region for the powder and NTs, the NWs exhibited a fairly strong emission band at 465 nm. We recorded the PL spectra of a single NW and a single NT by using a spectrometer coupled to a dark-field microscope system fitted with a halogen lamp (Figure S6). The NW exhibited strong blue emission centered at 465 nm. The inset of Figure 2b shows a dark-field microscope image of a single cyclo-FF NW, from which blue emission is clearly seen. We investigated the Raman properties of a single peptide NW by using polarized Raman microscopy on a single NW. The positions of the observed NW Raman bands are identical to those of NTs,[29,30] and the Raman bands of a single NW are distinctly observed only when the incident light is polarized parallel to the NW axis (Figure 3). The strong polarization dependence of the Raman bands of the FF NW is related to a shape effect.[31] A locally induced electric field within a NW decreases when the diameter of the NW is less than the wavelength of the laser light,[32] thus explaining the reduced Raman intensity when the polarization is perpendicular to the peptide NW axis.

The electric transport properties of a single cyclo-FF NW were also measured: a single NW was positioned between Pt

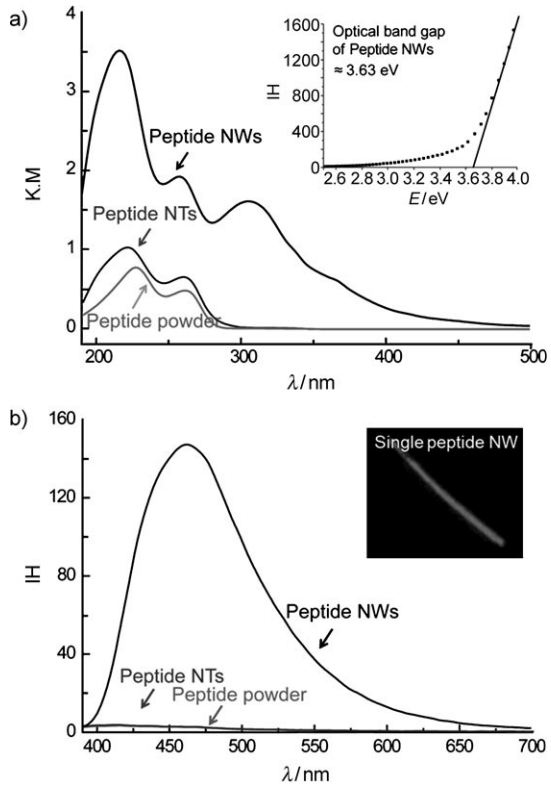

Figure 2. a) DRS curve; b) PL spectra of peptide powder, linear-FF NTs, and cyclo-FF NWs. The NWs exhibit a fairly strong emission band near 465 nm on excitation with light with a wavelength of 367 nm. The NTs and the powder show similar PL, which is much weaker than that of the NWs in the visible region. The inset in (a) shows an estimation of the optical band gap of the NWs. The inset in (b) shows a dark-field microscope image of a single NW recorded on a spectrometer coupled to a dark-field microscope system fitted with a halogen lamp, and the image shows strong blue emission from the NW (see Figure S5).

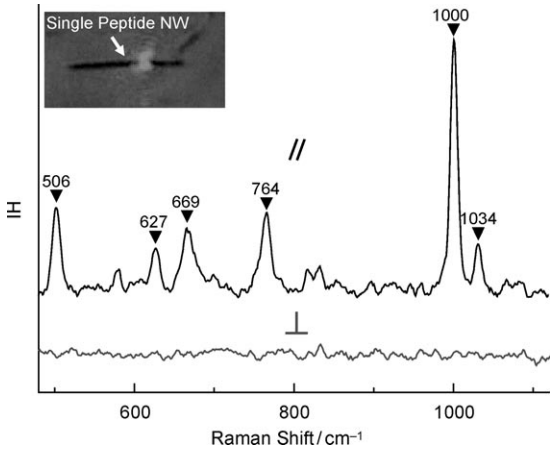

Figure 3. Polarized Raman microscopy of a single cyclo-FF NW with the polarization of the incident laser beam parallel (||) and perpendicular (⊥) to the NW axis. The peptide NW was illuminated by a He-Ne laser operating at a wavelength of 632.8 nm. The inset shows that the incident light (ca. 500 nm diameter) is focused on the center of the single NW. The NW Raman bands were observed only when the incident light was polarized parallel to the NW axis (top spectrum) and disappeared when the light was perpendicularly polarized (lower spectrum).

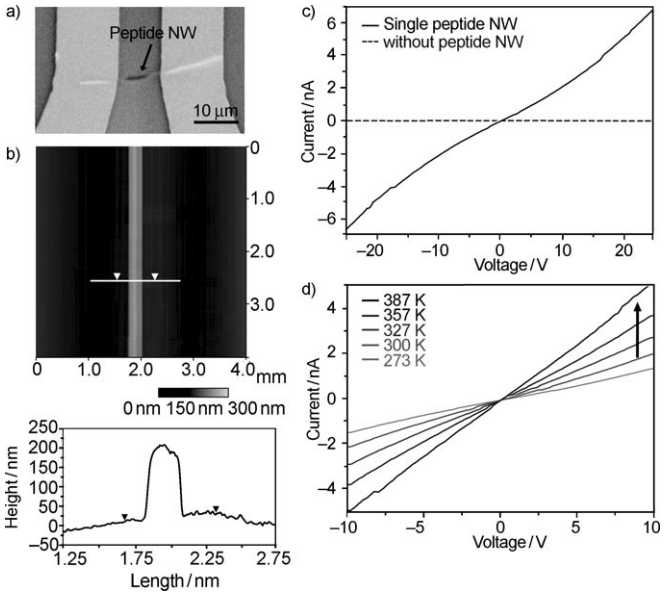

Figure 4. a) SEM image; b) AFM image and section analysis of a single cyclo-FF NW deposited between Pt electrodes, and characteristic current–voltage (*I–V*) curves of an orthorhombic peptide NW at c) 300 K and d) various temperatures. In (c), The *I–V* characteristics of the single NW (solid line) show a symmetrical behavior. When no NW was between the Pt electrodes (dotted line), the characteristic *I–V* curve was not observed.

electrodes that were prefabricated with a gap of 10 μm (Figure 4a,b). Platinum was deposited on both ends of the NW for electrical contact by using a focused ion beam. A symmetrical characteristic *I–V* curve indicates a Schottky-like barrier at the interface of the Pt and the NW at room temperature (Figure 4c). Figure 4d shows the temperature-dependent *I–V* characteristics of a cyclo-FF NW. The current increased as the temperature was increased from 273 K to 387 K under a fixed voltage. This behavior shows a typical semiconductor resistivity–temperature relationship. The *I–V* characteristics of the NW were stable over several potential cycles. The electric transport property observed for the cyclo-FF NW is quite striking compared to the insulating properties of linear-FF NTs self-assembled in aqueous solution.[28,33] Further studies are needed to unveil the detailed electrical transport mechanism in relation to the structure and surface properties of cyclo-FF NW.

In summary, semiconducting, blue-luminescent, and single-crystalline cyclo-FF NWs have been synthesized by vapor-phase self-assembly. The NWs are well-faceted with smooth surfaces, are orthorhombic crystals, and exhibit strong luminescence at 465 nm. Furthermore, electric-transport measurements reveal that the cyclo-FF NW possesses semiconducting properties. These results should open up new possibilities for employing the self-assembly of biological molecules in the fabrication of nanoelectronic and optical devices.

Received: June 7, 2010
Revised: November 16, 2010
Published online: December 23, 2010

Keywords: electron transport · nanostructures · peptides · photoluminescence · self-assembly

[1] S. Zhang, *Nat. Nanotechnol.* **2003**, *21*, 1171 – 1177.
[2] G. M. Whitesides, J. P. Mathias, C. T. Seto, *Science* **1992**, *254*, 1312 – 1319.
[3] S. Fernandez-Lopez, H. Kim, E. C. Choi, M. Delgado, J. R. Granja, A. Khasanov, K. Kraehenbuehl, G. Long, D. A. Weinberger, K. M. Wilcoxen, M. R. Ghadiri, *Nature* **2001**, *412*, 452 – 455.
[4] J. D. Hartgerink, E. Beniash, S. I. Stupp, *Science* **2001**, *294*, 1684 – 1688.
[5] Y. Xuehai, P. Zhu, J. Li, *Chem. Soc. Rev.* **2010**, *39*, 1877 – 1890.
[6] X. Gao, H. Matsui, *Adv. Mater.* **2005**, *17*, 2037 – 2050.
[7] I. Hamley, *Angew. Chem.* **2007**, *119*, 8274 – 8295; *Angew. Chem. Int. Ed.* **2007**, *46*, 8128 – 8147.
[8] L. Adler-Abramovich, M. Reches, V. L. Sedman, S. Allen, S. J. B. Tendler, E. Gazit, *Langmuir* **2006**, *22*, 1313 – 1320.
[9] N. Kol, L. Adler-Abramovich, D. Barlam, R. Z. Shneck, E. Gazit, I. Rousso, *Nano Lett.* **2005**, *5*, 1343 – 1346.
[10] J. S. Lee, J. Ryu, C. B. Park, *Soft Matter* **2009**, *5*, 2717 – 2720.
[11] J. Ryu, C. B. Park, *Angew. Chem.* **2009**, *121*, 4914 – 4917; *Angew. Chem. Int. Ed.* **2009**, *48*, 4820 – 4823.
[12] J. Ryu, C. B. Park, *Adv. Mater.* **2008**, *20*, 3754 – 3758.
[13] X. H. Yan, Y. Cui, Q. He, K. W. Wang, J. B. Li, *Chem. Mater.* **2008**, *20*, 1522 – 1526.
[14] C. H. Gorbitz, *Chem. Commun.* **2006**, 2332 – 2334.
[15] C. H. Görbitz, *Chem. Eur. J.* **2001**, *7*, 5153 – 5158.
[16] J. Kim, T. H. Han, Y.-I. Kim, J. S. Park, J. Choi, D. G. Churchill, S. O. Kim, H. Ihee, *Adv. Mater.* **2010**, *22*, 583 – 587.
[17] L. Adler-Abramovich, D. Aronov, P. Beker, M. Yevnin, S. Stempler, L. Buzhansky, G. Rosenman, E. Gazit, *Nat. Nanotechnol.* **2009**, *4*, 849 – 854.
[18] J. Li, T. B. Brill, *J. Phys. Chem. A* **2003**, *107*, 8575 – 8577.
[19] C. J. Balibar, C. T. Walsh, *Biochemistry* **2006**, *45*, 15029 – 15038.
[20] Y. Qian, M. H. Engel, S. A. Macko, S. Carpenter, J. W. Deming, *Geochim. Cosmochim. Acta* **1993**, *57*, 3281 – 3293.
[21] Y. Zhu, M. Tang, X. Shi, Y. Zhao, *Int. J. Quantum Chem.* **2007**, *107*, 745 – 753.
[22] M. Gdaniec, B. Liberek, *Acta Crystallogr. Sect. C* **1986**, *42*, 1343 – 1345.
[23] M. S. Yoon, I. C. Hwang, K. S. Kim, H. C. Choi, *Angew. Chem.* **2009**, *121*, 2544 – 2547; *Angew. Chem. Int. Ed.* **2009**, *48*, 2506 – 2509.
[24] M. Reches, E. Gazit, *Science* **2003**, *300*, 625 – 627.
[25] M. Reches, E. Gazit, *Nat. Nanotechnol.* **2006**, *1*, 195 – 200.
[26] E. Cortez, J. Laane, *J. Mol. Struct.* **1995**, *346*, 41 – 49.
[27] E. J. Mihalyi, *Chem. Eng. Data* **1968**, *13*, 179 – 182.
[28] R. Takahashi, H. Wang, J. P. Lewis, *J. Phys. Chem. B* **2007**, *111*, 9093 – 9098.
[29] G. Singh, A. M. Bittner, S. Loscher, N. Malinowski, K. Kern, *Adv. Mater.* **2008**, *20*, 2332 – 2336.
[30] S. Stewart, P. M. Fredericks, *Spectrochim. Acta Part A* **1999**, *55*, 1615 – 1640.
[31] T. Livneh, J. Zhang, G. Cheng, M. Moskovits, *Phys. Rev. B* **2006**, *74*, 035320.
[32] H. M. Fan, X. F. Fan, Z. H. Ni, Z. X. Shen, Y. P. Feng, B. S. Zou, *J. Phys. Chem. C* **2008**, *112*, 1865 – 1870.
[33] J. Castillo, S. Tanzi, M. Dimaki, W. Svendsen, *Electrophoresis* **2008**, *29*, 5026 – 5032.

